

1 Foraging fruit flies mix navigational and learning-based 2 decision-making strategies

3 Sophie E. Seidenbecher^{1,2}, Joshua I. Sanders³, Anne C. von Philipsborn^{1,2},
4 Duda Kvitsiani^{1,2,*}

5 ¹ Danish Research Institute of Translational Neuroscience - DANDRITE,
6 Nordic-EMBL Partnership for Molecular Medicine.

7 ² Aarhus University, Department of Molecular Biology & Genetics, Denmark.

8 ³ Sanworks LLC, Stony Brook, NY 11790, United States.

9 * kvitsi@dandrite.au.dk

10 Abstract

11 Animals often navigate environments that are uncertain, volatile and com-
12 plex, making it challenging to locate reliable food sources. Therefore, it is
13 not surprising that many species evolved multiple, parallel and complementary
14 foraging strategies to survive. Current research on animal behavior is largely
15 driven by a reductionist approach and attempts to study one particular aspect
16 of behavior in isolation. This is justified by the huge success of past and current
17 research in understanding neural circuit mechanisms of behaviors. But focus-
18 ing on only one aspect of behaviors obscures their inherent multidimensional
19 nature. To fill this gap we aimed to identify and characterize distinct behavioral
20 modules using a simple reward foraging assay. For this we developed a single-
21 animal, trial-based probabilistic foraging task, where freely walking fruit flies
22 experience optogenetic sugar-receptor neuron stimulation. By carefully analyz-
23 ing the walking trajectories of flies, we were able to dissect the animals foraging
24 decisions into multiple underlying systems. We show that flies perform local
25 searches, cue-based navigation and learn task relevant contingencies. Using
26 probabilistic reward delivery allowed us to bid several competing reinforcement
27 learning (RL) models against each other. We discover that flies accumulate
28 chosen option values, forget unchosen option values and seek novelty. We
29 further show that distinct behavioral modules -learning and navigation-based
30 systems- cooperate, suggesting that reinforcement learning in flies operates
31 on dimensionality reduced representations. We therefore argue that animals
32 will apply combinations of multiple behavioral strategies to generate foraging
33 decisions.

34 Introduction

35 Modular organization of biological systems provides species with flexibility to inde-
36 pendently evolve distinct biological functions [1]. Hierarchical organization on the
37 other hand enables coordination of multiple functions to serve common goals. Seven
38 decades ago Nikolaas Tinbergen has recognized that animal behaviors show ample ev-
39 idence of modularity and hierarchy [2]. Both experimental and theoretical work have
40 addressed why and under what conditions distinct behavioral modules or strategies
41 may emerge.

42 Spatial and temporal variations, changes in both mean and variance of quality
43 and quantity of food patches, pose a serious challenge to all foraging animals to
44 optimize decisions. Successful strategies must therefore be shaped to accommodate
45 environmental uncertainty and volatility. A large body of evidence suggests that
46 animals and humans are able to track such changes in the environment [3, 4]. In
47 theory, animals could optimize food gathering performance by using trial and error
48 and incorporate simple forms of reinforcement learning (RL) [5] to deal with variability
49 in their habitats. Indeed, the RL framework has been successfully used to explain
50 animal behavior in many learning paradigms [6]. The utility of the RL framework
51 lies in its ability to extract decision variables that are not directly observable to
52 the experimenter. Furthermore, using model comparison one can select the best
53 predictive and generative RL model and see what behavioral strategies are used by
54 animals. For example, according to standard Rescorla-Wagner RL models [6] the
55 unchosen option values are "frozen" and updated only after the animal samples that
56 option. Alternative RL models assume that unchosen option values decay (the animal
57 forgets) and are updated only when the animal chooses that option. Theoretical
58 and experimental evidence suggest that flies use the latter strategy to learn new
59 associations [7, 8]. However, direct predictive and generative tests that would bid
60 several RL models against each other are missing.

61 Besides environmental variability in their natural habitats animal are exposed to
62 novel stimuli or new behavioral contingencies (i.e. old actions that lead to new,
63 unexpected outcomes). According to theoretical work [9] foraging animals should
64 explore novelty since this will lead to faster learning of behavioral contingencies.
65 Electrophysiological recordings [10] as well as behavioral studies in mammals [11]
66 have shown that novelty itself is rewarding. These observations can be explained
67 by the class of RL models that explicitly incorporate novelty bonuses in the value
68 update process [12]. Although fruit flies display behavioral and electrophysiological

69 signatures of novelty [13], it remains to be seen whether novelty elicits behaviorally
70 rewarding effects in flies.

71 Simple forms of RL-based strategies are very effective when the space of potential
72 actions is small, but they become energetically very costly when this space grows,
73 like in natural foraging scenarios. Therefore, alternative to trial-and-error learning
74 animals can save time and effort by using short-cuts derived from already estimated
75 or learned schemas [14] and spatial representations [15].

76 One estimation strategy is based on forms of navigation [16, 17, 18]. If a landmark
77 can be associated with a food source, locating it can be achieved using representation
78 of external cues [17]. In the absence of landmarks, animals use idiothetic cues [19, 16,
79 18] to locate previously visited rewarding locations. Furthermore, since most food in
80 nature is not uniformly distributed, but rather occurs in patches, another strategy to
81 maximize energy intake is to perform local searches around recently discovered food
82 items. Indeed, local searches emerge in insect navigation when animals encounter
83 natural [20] or fictive food sources [18, 21, 22].

84 Thus, navigation-based and learning strategies may complement each other by
85 balancing efficiency and adaptability in a foraging context, to maintain and improve
86 an animal's fitness. Here we examine whether multiple behavioral strategies are
87 concurrently applied by animals and how they interact. For this we designed a single-
88 animal, trial-based probabilistic reward foraging assay in fruit flies. By dissecting the
89 flies' behavior into multiple behavioral modules we observed that these animals mix
90 learning and navigation-based systems to form foraging decisions. This suggests a
91 mechanism by which the insect brain solves the curse of dimensionality and distal
92 reward problem faced by simple, model-free RL systems [15]. Our results imply that
93 even in a most reduced setup, such as our plain linear-track arena, single behavioral
94 strategies cannot be completely isolated from the ecologically sensible mixture.

95 Results

96 Optogenetic stimulation of sugar receptor neurons induces 97 place preference

98 We set up a single-fly, closed-loop optogenetic stimulation assay where the fly is
99 walking in a linear track arena. The trigger and reset zones are placed at each end of
100 the arena (Fig. 1A). Single pulses of optogenetic stimulation with a fixed probability
101 are delivered only when the fly crosses the reset and trigger zones as described in the

102 inset in Fig. 1A. Thus, simply staying in the trigger zone will not provide optogenetic
103 stimulation. Similar to previous studies [26, 22, 18], we observed clear effects of the
104 light stimulation on behavior.

105 First, we looked at how kinematic variables evolved as a function of stimulation
106 frequency. Since our setup can be seen as one-dimensional, we first focused our
107 analysis on the walking traces along the x-axis (long axis). Optogenetic stimulation
108 induced observable changes in the flies' locomotion. While unstimulated, flies cover
109 the whole space of the arena by walking back and forth, which is shown for one
110 example fly in Fig. 1B (magenta traces). In contrast, the stimulation induced a
111 preference for the stimulation side (Fig. 1B, green traces). By testing stimulation
112 probabilities from 0 - 100%, we show that place preference (measured by occupancy
113 probability of x positions) positively correlates with the stimulation frequency, both
114 on the level of the individual fly (Fig. 1C) and the population (Fig. 1D). The 5
115 % population occupancy distribution (Fig. 1D) is very similar to unstimulated and
116 genetic controls, showing that the low stimulation probability is not enough to induce
117 a significant place preference. We observe a temporal decay of the place preference
118 (Fig. 1E) with a probability dependent magnitude. This indicates a saturation or
119 behavioral adaptation effect in response to the optical stimulation.

120 To quantify the flies' preference for the stimulation side we compared the flies'
121 zone preference index in Fig. 1F. Preference indices were computed from the occu-
122 pancy distributions for each zone (within the reset zone boundaries), using

$$PI = \frac{\text{Zone 1 Occupancy} - \text{Zone 2 Occupancy}}{\text{Zone 1 Occupancy} + \text{Zone 2 Occupancy}}, \quad (1)$$

123 which produces preference index values between -1 and 1 , meaning strong zone
124 2 or strong zone 1 preference, respectively, and indifference at $PI=0$. There is a
125 positive correlation of the stimulation probability and zone preference index, which is
126 significant at stimulation probability of 15% or higher. All stimulated genetic control
127 animals had preference indices around 0, proving that this preference effect doesn't
128 stem from simple attraction to the light. To test if flies had an intrinsic preference
129 for one side of the arena that is independent of the optical stimulation, we performed
130 double sided stimulation experiments. We observe similar levels of occupancy and
131 place preference with these flies (Fig. S2A,B).

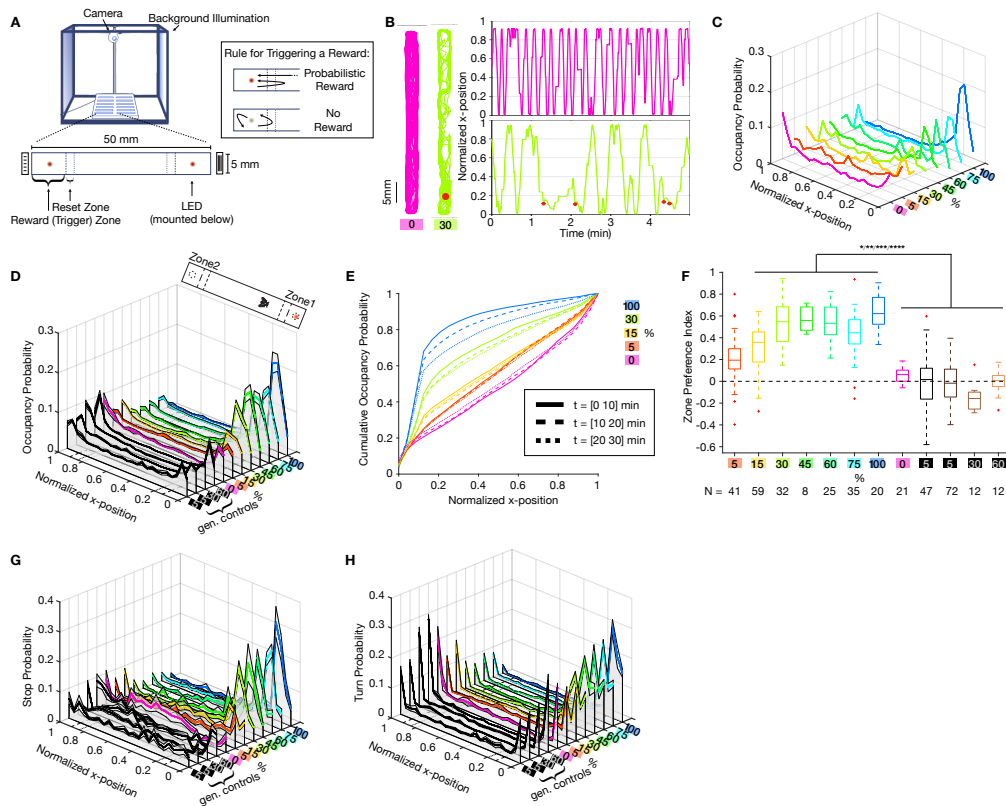


Figure 1: Place preference as a function of *Gr5a*-receptor-neuron stimulation. **A** Single-fly optogenetic foraging setup. A system of 12 linear track arenas is placed in a behavior box with uniform white background illumination and monitored by a webcam from above. Each arena consists of two LEDs ($\lambda = 624$ nm) mounted from below. Reset and trigger zones (short and long dash) are not visible to the flies. Each trigger zone is marked by black and white stripe patterns with different orientations on each side. Inset: Rule for triggering a probabilistic flash of light. Light is triggered only when the fly enters the reset and the reward zones in that order. **B** Left: Two dimensional walking traces of an unstimulated example fly (magenta) and 30% probability stimulated example fly (green). Light stimulation was delivered to only one side of the arena, here marked with red dot. Right: One dimensional walking trace over time of the same example flies. Stimulation events are marked with red dots. **C** Occupancy distribution of example individuals from 0-100% stimulation conditions. **D** Occupancy distribution of fly populations that experienced the same stimulation probabilities as in **C**. Solid lines: Mean, shaded regions around mean: \pm SEM. Genetic controls don't express Chrimson. **E** Cumulative occupancy distribution over 10 minute intervals across time. Higher stimulation probability leads to a decrease of zone preference over time. **F** Zone preference index of stimulated fly populations and genetic controls. Equal zone preference at preference index value 0 marked with black dashed line. Positive values indicate preference for zone 1 (stimulated) and negative values for zone 2. Stimulated flies have a significant zone preference of the stimulated zone over the unstimulated zone. (*: $p < 0.05$; **: $p < 0.01$; ***: $p < 0.001$, Kruskal-Wallis test with multiple comparisons). **G** Stop distribution in the arena for the fly populations. Solid lines: Mean, shaded regions around mean: \pm SEM. For definitions of stops and turns refer to materials and methods **H** Turning distribution for the fly populations. Solid lines: Mean, shaded regions around mean: \pm SEM.

132 **Optogenetic stimulation of sugar receptor neurons triggers** 133 **local search**

134 The optical stimulation does not affect the average speed of the fly, but has an effect
135 on speed distribution and the time duration the fly lingers around the stimulation zone
136 (Fig. S1A, S2C,D). Thus, place preference that flies show can be due to an increase in
137 the frequency of stop events that happens upon optical stimulation. We define stops
138 as the speeds below a set threshold level, determined by the resolution of the camera
139 (for precise definition of stops refer to the materials and methods section). The
140 frequency of stops increases with stimulation probability (Fig. 1G). Increase in stop
141 events was accompanied by an increase in turning events around the reward location
142 (Fig. 1H). Due to the fact that the fly arena is effectively one dimensional turns
143 are defined as velocity sign changes and indicate reversal of walking direction. The
144 probability of turns increases upon optical stimulation on the stimulated side, while
145 it decreases for the unstimulated side(Fig. 1H). Compared to the control population
146 the turn frequency surpasses that at the arena walls seen in the control populations
147 (Fig. 1H) . Therefore, we concluded that local searches operationally defined as
148 stops and turns signal local search behavior as shown in previous studies [22, 18] and
149 suggest that the stimulation was rewarding [27].

150 Next we asked whether local searches simply occur as a reaction to the opto-
151 genetic stimulation (innate behavioral responses) or whether they show adaptation
152 to the probabilistic structure of environment. We looked at the two-dimensional
153 walking traces and computed the angular distributions of the trajectories in zone 1
154 (Fig. S3C). While they were significantly different for stimulated vs non-stimulated
155 events for each probability condition, the angular distributions on stimulated trials
156 across probability conditions were not. The same was true for probability conditions
157 of 5 and 15% (not shown here). Together, this suggests that local searches emerge
158 when flies receive optogenetic stimulation and they do not show any adaptation to
159 different probability conditions.

160 **Flies accumulate action value over trials**

161 In addition to initiating local searches, the animals should also return to the stimula-
162 tion area, if the stimulation was rewarding. To measure this, we split the continuous
163 walking trajectories into discrete trials. We defined a trial to be the time between
164 two crossings of the same reset zone and the accompanying reward zone from the
165 same direction, see Fig. 2A. This means that within a trial, the fly will have visited

166 a reward zone, made the choice to either return to the same zone again without
167 reaching the other zone (return decision), or to sample the other reward zone before
168 returning. Trials also differed in whether or not the fly was rewarded when it entered
169 the reward zone. In this way, we created a sequence of binary events given by a prob-
170 abilistic reward followed by a binary choice to return or not. Fig. 2B shows the return
171 probability for all trials (rewarded and unrewarded) to each zone (one and two) for
172 all tested probability conditions. In all stimulated conditions, returns to the rewarded
173 zone were significantly increased over returns to the unrewarded zone, which was not
174 the case for the unstimulated and genetic controls (Fig. 2B, inset).

175 The experienced reward rate and set reward probabilities may differ due to the
176 stochastic nature of the reward delivery. We also show a positive correlation of
177 returns with the experienced reward rate Fig. 2C.

178 Since we defined returns as an additional behavioral read-out, one obvious ques-
179 tion emerges: Are returns part of local search behavior or do they constitute a sepa-
180 rate behavioral module? To answer this question we looked at the temporal dynamics
181 of returns and local searches (Fig. S3A,B) and observed that while local searches are
182 tightly locked to stimulation onset and settle to baseline within 10 – 15 seconds,
183 returns on the other hand are mostly occurring between 15 – 25 sec. While there
184 occasionally is some overlap, the majority of returns happens temporally separated
185 from the local search behavior.

186 The trend in Fig. 2B,C suggested that flies accumulate action (return) values over
187 rewarded trials as proposed by a previous study [22]. This effect of rewards on choices
188 to return to the rewarded location was also seen on the strength of correlations be-
189 tween rewards and choices (Fig. S4B) for different probability conditions. However,
190 our optical stimulation protocol can sensitize or desensitize directly activated neurons
191 to subsequent stimulations. This can hinder behavioral interpretations of such ma-
192 nipulation experiments. Indeed, we saw strong behavioral evidence of desensitization
193 over time in high probability stimulation sessions. The desensitization effects were
194 most pronounced in the 100% stimulation case (Fig. S4A) and were absent at lower
195 probabilities both for single (Fig. S4A) and double sided stimulation (Fig. S2G). This
196 makes it look as if animals show diminishing action values. The probabilistic reward
197 delivery allowed us to avoid this problem and analyze how returns changed as a func-
198 tion of reward probability, on trials where animals had not been subjected to optical
199 stimulation. Our data shows that as reward probability and reward rate increased,
200 returns scaled up to the rewarded location on non-rewarded trials compared to the
201 non-rewarded locations (Fig. 2D). Thus, there is evidence that flies are accumulating

202 an internal value of actions as a function of reward rates.

203 To look more directly into value accumulation we used logistic regression analysis
204 to see how past rewards contributed to current choices and computed the reward
205 effects (reward kernel) on return choices [28]. We show that immediate rewards
206 had the strongest effect on current choices while rewards further back in the trial
207 history had smaller contributions (Fig. 2E). The same effects were seen with two-
208 sided optical stimulation (Fig. S2E, left and middle panels and Fig. S2F). Based on
209 our analysis we concluded that flies mostly rely on current rewards to make choices,
210 but also incorporate rewards into their choices that happen further back in trials. The
211 simulation of fly responses to only immediate rewards generates very steep reward
212 kernels (Fig. S4C) unlike the ones we see in the animal data. This is consistent with
213 the idea that flies accumulate reward value over trials.

214 In some of the reward foraging studies using a probabilistic reinforcement struc-
215 ture [28, 29] not only rewards, but also past choices contribute to the animals' current
216 choices. This is sometimes termed decision inertia [30]. To test if flies also exhibited
217 decision inertia we regressed current choices on past choices. Our analysis failed to
218 detect any effects of past returns on current returns (Fig. 2F, Fig. S2E, right panel).

219 **Reinforcement learning models that use forgetting and learn-** 220 **ing rates capture fly behavior**

221 Regression analysis of rewards and returns revealed that immediate rewards had
222 strongest effects on choices. However this analysis did not distinguish how flies update
223 the value of chosen unrewarded vs unchosen option trials (refer to the methods section
224 for details). To see how unchosen option values are updated, we modeled the choice
225 behavior within a reinforcement learning framework by comparing three RL models
226 that use different update rules for unchosen options. One model freezes the value,
227 one forgets the value with the same parameter as the learning rate α and the third
228 forgets the value with a separate forgetting parameter α_F . Examples of the evolution
229 of the value over trials for all three models are depicted in Fig. 3A. To account for the
230 fact that the flies have a baseline return probability below 50%, we included a bias
231 parameter. Model selection using the Akaike information criterion (AIC) score [53], a
232 measure that describes how well a model fits the data by accounting for the number
233 of parameters (Fig. S5A), as well as predictive (Fig. S5C,D) and generative tests
234 (Fig. S5E,F) slightly favored the second model which we termed forgetting-Q model,
235 or FQ. The best-fit parameter values show a high variability across flies and similar

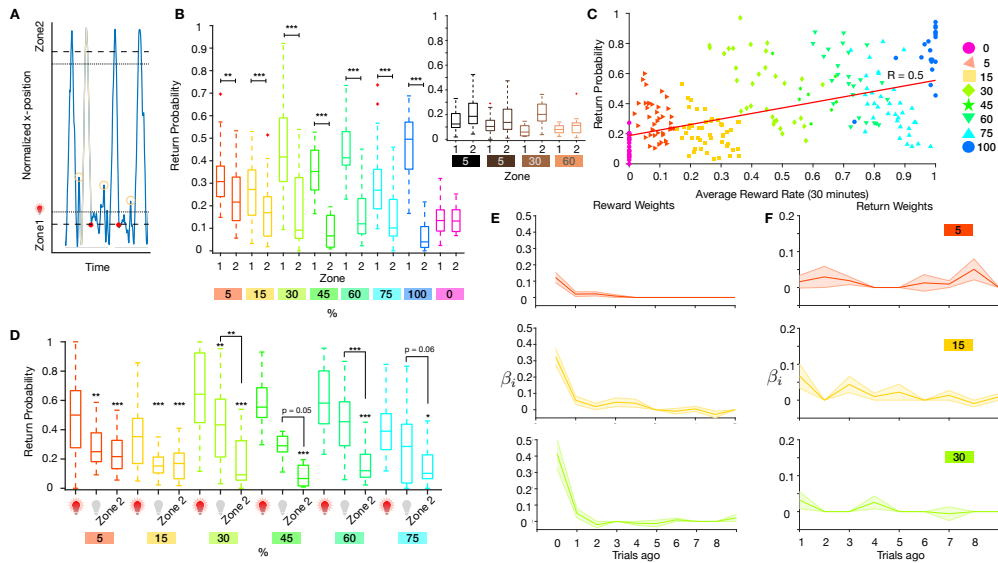


Figure 2: Flies return to optogenetic stimulation site **A** Definition of a trial (highlighted trace) and a return (yellow circle). Walking trace of one example fly over time in blue. Zone boundaries marked with dashed and dotted lines. Returns are defined as trajectories that leave the reward and reset zone and return to the same reward zone, before reaching the other side's reset zone boundary. **B** Total return behavior per probability condition to zones 1 and 2. (*: $p < 0.05$; **: $p < 0.01$; ***: $p < 0.001$, Mann-Whitney U test) Inset: Return behavior to both zones for genetic controls not expressing Chrimson. **C** Return probability versus average reward probability over 30 minutes. Black line: Pearson correlation, $R = 0.5$, $p = 1e-16$ (Robust Correlation package by [32]). **D** Return behavior on rewarded trials (red light bulb), unrewarded trials (grey light bulb) and always unrewarded zone 2. (*: $p < 0.05$; **: $p < 0.01$; ***: $p < 0.001$, Kruskal-Wallis test with multiple comparisons). **E** Logistic regression against the reward history. Solid lines: Population averages, shaded regions: \pm SEM. **F** Logistic regression of the return choices in the 5%, 15% and 30% condition against choice history for 10 trials into the past. Solid lines: Population average, shaded regions: \pm SEM.

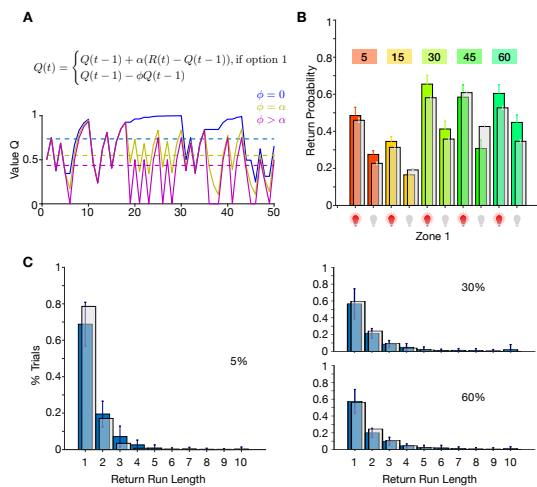


Figure 3: Reinforcement learning captures the probability dependent returns upon rewards. **A** Top: Update rule for the value. The three models differ in the choice of ϕ . Bottom: Examples of value evolution over trials for each choice of ϕ . RW model: blue, FQ model: yellow, FQ $_{\alpha_F}$ model. **B** Generative test of the FQ model. Return probability separated by stimulated (red light bulb) and unstimulated (grey light bulb) trials to the rewarded zone per probability condition for the data (colored) and the model (grey). Bars: Population mean \pm SEM. **C** Return choice run length histogram for population 5, 30, 60% fly data (blue) and the model (100 simulations, grey). Bars: Mean \pm SEM. Run lengths are defined as consecutive returns to the same side.

236 mean values across experimental conditions (Fig. S5B). Predictive testing of the best-
 237 fit FQ model on the data yielded rather poor overall accuracy (Fig. S5C,D). However,
 238 F_1 accuracy reached 80% when the model was fit on data that had roughly equal,
 239 or higher, numbers of returned to not-returned trials. Nevertheless, under generative
 240 testing the model was able to produce similar return probabilities as the flies (Fig. 3B)
 241 and reproduced return run lengths (Fig. 3C). We defined return run lengths as the
 242 number of consecutive returns to the same side. The same analysis performed on flies
 243 with two-sided stimulation also favored the FQ model (Fig. S2H) that showed good
 244 predictive (Fig. S2J) and generative performance (Fig. S2K). However, we observed
 245 a much smaller spread of the FQ parameter values (Fig. S2I). We think that this
 246 discrepancy stems from the data limitation for one-sided stimulation trials.

247 Fruit flies rely on cue-guided navigation in addition to trial- 248 and-error learning to make foraging decisions

249 Central to all RL algorithms is that actions need to be executed before an associative
 250 learning process takes place. Alternatively, animals can execute novel actions guided
 251 by explicit representations of space and rewarded (or punished) locations [17]. To test
 252 if flies also made representation-guided choices we looked at the return probability on
 253 the very first rewarded trials. Note that due to the nature of our task design (Fig. 1A)
 254 return behavior is not required to deliver first rewards, as flies will experience rewards
 255 even if they walk back and forth the entire arena. Thus, the first rewarded trials
 256 naturally dissociate actions (returns) from outcomes, contrary to how it is done

257 in classical operant training protocols [31]. We observed that flies returned above
258 chance level on the very first rewarded trials (Fig. 4A).

259 In our foraging assay the walls of the arena were covered with stripes that can
260 aid the flies to navigate and locate the rewarded locations. In the studies by [16, 22]
261 it was shown that visual or tactile cues in addition to idiothetic cues help animals
262 to locate the rewards. This suggests that fruit flies in our assay used cue-based
263 navigation (explicit or implicit) in addition to trial-and-error learning (simple forms
264 of RL-based learning) to form choices.

265 **Novelty increases action values**

266 We observed to our surprise the reward probability dependence of the returns on
267 the first rewarded trials (Fig. 4A). One possible explanation could be that the flies
268 were sensitive to the timing of the first reward in the session. To further elucidate
269 behavioral mechanisms that drive this form of adaptation we looked at the delay of
270 the first rewards from the start of the session using both trial (Fig. 4B,E) and time-
271 based analysis (Fig. 4C,D). Both measures showed a similar trend of decreased return
272 probability with increased delay. This analysis suggests that optogenetic rewards
273 become more attractive when they are delivered in novel environment (fly arena and
274 its edges are novel at the beginning of the behavioral session). We observed the
275 same effect of the first rewarded trial on return probability when both sides were
276 used to deliver optogenetic stimulation (Fig. S2D). The novelty of the arena on its
277 own also exerted rewarding effects on flies as control flies that never experienced
278 rewards showed above baseline level of returns that decreased to baseline (Fig. 4D,E,
279 insets). This decay was fast as no change in returns were observed on first and later
280 trials (Fig. 4C, magenta circles connected with grey line) on a time-scale of minutes.

281 Our previous analysis suggested that the action value accumulates as the num-
282 ber/probability of rewarded trials increases (Fig. 2D). If so, the timing of the first
283 rewarded trial may have affected the subsequent return probability as the action value
284 should be higher for early vs later occurring first rewards. For this we looked at the
285 return probability on all subsequent trials when first rewards happened within the
286 first 3 trials (this number was chosen since the return probability does not change
287 if the fly is rewarded after the 3rd trial (Fig. 4E)) or later (Fig. 4F). We could not
288 detect a significant difference in return probability between these groups, suggesting
289 that except for the first few trials the behavior of the animal was not affected by
290 the timing of the first rewards. There could be individual differences to novelty that

291 may indicate the flies' sensitivity to rewards in general. Therefore, we separated flies
292 that showed return on first rewarded trial from flies that did not return on the first
293 rewarded trial and looked at the return probability on all subsequent rewarded trials
294 (Fig. 4G). We show that return behavior on the first rewarded trial is a good predictor
295 of future returns and may reflect individual differences among flies.

296 To formally account for the observed responses of flies on the first rewarded trials
297 we incorporated this in our RL models and assumed that option values (in our case
298 zone 1 and zone 2 of the arena) are not set to zero initially (due to novelty), but rather
299 start with some default positive value that over time decays (Fig. 4H). Note, that
300 this simple model qualitatively explains novelty attraction in control flies that never
301 experienced optical stimulation. We also tested if such RL model could correctly
302 predict flies returns to first rewards. Our modified FQ RL model indeed generated
303 similar return probabilities (Fig. 4I), explaining novelty mediated reinforcing effects
304 of optical stimulation.

305 **Cooperation of learning and navigation-based systems**

306 After discovering that flies apply both navigation and learning based strategies to
307 locate the optogenetic rewards, we asked how these two systems interact with each
308 other. Previous work [16] has shown that inbound paths of flies to their feeding sites
309 are more straight than outbound paths, suggesting that path integration mechanisms
310 help animals reach their feeding sites using shorter routes. Here we used a similar
311 approach and decided to look at how flies navigated towards and away from their
312 rewarded location as a function of accumulated value. We looked at the angular
313 distribution of walking paths on rewarded and non-rewarded trials as a function of
314 reward probability. The more curved a path is, the more uniform the corresponding
315 angular distribution gets, which translates into a higher angular distribution entropy
316 (Fig. 5A). First we noted that out-walking (walking away from the rewarded location)
317 paths generally had slightly higher spread in angular distribution compared to in-
318 walking paths (walking towards rewarded location) (Fig. 5B,C). This difference did
319 not reach statistical significance. We noted, however, a consistent trend in the
320 reduction of angular distribution of in-walking paths as a function of the reward
321 probability (Fig. 5D) ($p < 0.05$ for 5 and 15% reward probability compared with the
322 100% reward probability). Thus, flies choose to walk more straight paths towards
323 the rewarded locations as a function of reward value. Based on our results and the
324 published work we speculated how learning and navigation-based systems interact at

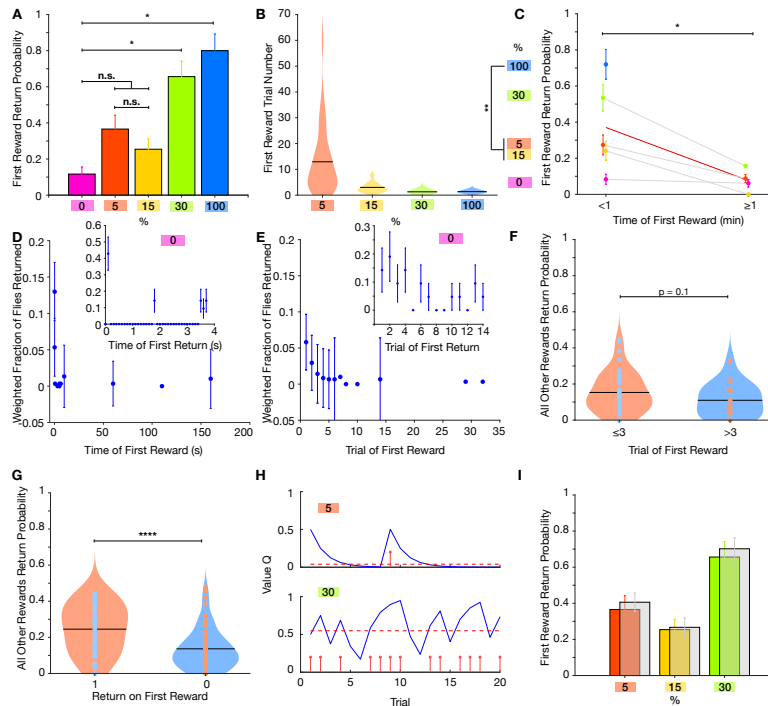


Figure 4: Returns on first reward **A** Return behavior upon first reward per probability condition. For unstimulated controls (0%, magenta) the return probability was computing for the first trial. (*: $p < 0.05$; pairwise Fishers exact test.) **B** First rewarded trial number per probability condition. Black lines: mean. **C** Return behavior upon first reward within the first minute of recording and after the first minute. Blue circles without a connecting grey line correspond to conditions where the first reward always happened within the first minute. Red line: average return probability. Magenta circles and dark grey line: unstimulated controls. Error bars: \pm SEM. (*: $p < 0.05$; **: $p < 0.01$; ***: $p < 0.001$, Kruskal-Wallis test with multiple comparisons and Welch's t-test). **D** Fraction of flies (independent of stimulation probability) that returned to a first reward within the first 200 s (time bins: 0.03 s between 0 and 1 s, 0.1 s between 1 and 9 s, 50s from 10 to 200 s and 100 s from 300 to 1000 s). Inset: Fraction of unstimulated flies that returned for the first time since the session start against time (time bins of 0.1 s). **E** Fraction of flies that returned to a first reward within in the first 30 trials. Inset: Fraction of unstimulated flies that returned for the first time against the trial index. **F** Return probability to all other rewarded trials when the first reward happened within the first 3 trials (orange violin) or after the first 3 trials (blue violin). **G** Return probability to all other rewarded trials depending on whether the fly returned upon the first reward (orange violin) or not (blue violin). (***: $p < 0.001$, Welch's t-test) **H** Two examples for the evolution of the RL value Q (blue curve) over trials. Upper figure: 5% stimulated fly. Lower figure: 30% stimulated fly. Red stems: stimulation events. Red dashed line: average value. **I** Transparent grey bars: RL model's prediction of first reward return rate. (Color bars as in **A**)

325 the neural level (Fig. 5E). We propose that dopamine mediated reward prediction
326 error assigns values to spatial representations (external or internal spatial cues stored
327 in the insect central complex [17, 33, 34] or mushroom bodies [35]). Thus, animals
328 do not have to learn entire action sequences and instead can compare values of
329 short-cuts to choose the better options. This effectively reduces the complexity of
330 the action-outcome contingencies during the learning process.

331 Discussion

332 We developed a single-fly, trial-based optogenetic reward foraging assay and discov-
333 ered that foraging decisions in fruit flies can be broadly categorized into navigational
334 and learning-based systems. Detailed analysis allowed us to discover distinct behav-
335 ioral modules: local searches, cue-based navigation, novelty seeking, learning and
336 forgetting processes. What is the biological function of these modules and how do
337 they interact with each other in the context of foraging decisions?

338 As previously described for natural rewards [36] the flies in our assay initiated
339 local searches as a function of experienced optogenetic stimulation, showing that
340 artificial stimulation of sugar receptor neurons recapitulated the natural behavioral
341 response in these animals. Looking at the temporal dynamics of local searches, we
342 see that they persist for roughly 10-15 seconds after a stimulation and do not show
343 any dependence on the frequency of the stimulation. This suggests that sweet-
344 taste induced local search is a hard-wired behavioral module. We speculate that this
345 behavioral module serves to anchor animals around recently discovered food items to
346 maximize the energetic gain from that source [37].

347 Local searches are a useful behavior once the animal has discovered a food source.
348 Finding a new food patch or returning to already discovered ones requires alternative
349 foraging strategies. In insects these strategies can arise either from representation-
350 based systems [19], using external or idiothetic cues, or learning action-outcome
351 contingencies [38, 31]. Clear separation of these two mechanisms requires monitor-
352 ing of animal behavior from the initial phase of learning to its stable performance.
353 By controlling reward delivery with optogenetic means, we were able to track the
354 animals' decisions to locate rewards on the very first trial. This excluded the possi-
355 bility of learning action-reward contingencies to guide animals' choices. Our results
356 demonstrate that fruit flies rely on representations to locate the rewarding sites, since
357 we saw a modulation of walking paths before and after receiving optical stimulation.
358 Representation-guided foraging decisions have a clear advantage over simple forms of

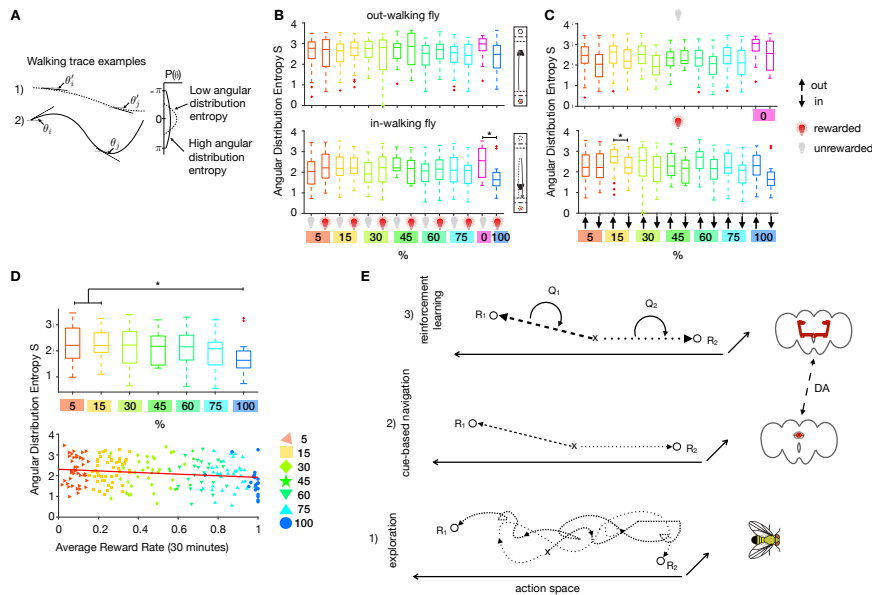


Figure 5: Interaction of navigation and learning systems during a foraging task **A** Sketch of path angular distribution analysis. The 'straighter' path 1) is characterized by a narrow angular distribution, while the more curved path 2) has a broader angular distribution. If the distribution is narrowly peaked, it has a smaller entropy S than a broader distribution. **B** Angular distribution entropy of in- and out-walking paths, on rewarded (red light bulb) and unrewarded (grey light bulb) trials. For out-walking (away from the rewarded zone, measured from the reset zone) trajectories, there is no difference between rewarded and unrewarded trials. For in-walking trajectories (from the position of return to the reset zone), the rewarded trials have a smaller entropy, corresponding to more straight paths. This is significant for 100% compared to unstimulated controls (*: $p < 0.05$, Kruskal-Wallis test with multiple comparisons). **C** Same data as in **B** but sorted by unrewarded (top) and rewarded (bottom) trials. (*: $p < 0.05$, Kruskal-Wallis test with multiple comparisons). **D** There is a trend of more straight in-walking after a reward (indication of path integration) with increased reward probability. Top figure: only rewarded trials from **B** bottom (*: $p < 0.05$, Kruskal-Wallis test with multiple comparisons). Bottom figure: Same data plotted against each flies experienced average reward rate. Red line: Pearson correlation, $R = -0.18$, $p = 0.005$ (Robust Correlation package by [32]). **E** Proposed schematic of the interaction of navigation and learning systems in a foraging task. 1) A foraging fly starts navigation in a new environment with the sequence of actions (dashed) that leads to reward R_1 . After that, the fly continues to forage on a path (dotted) experiencing another reward R_2 . 2) After leaving R_2 , the fly can make a decision to return to the R_1 or R_2 rewarded site via the already executed and rewarded path (dashed or dotted) or, using cue-based navigation, travel on shortcuts to the rewarded locations. 3) Combined with reinforcement learning, values are assigned to those shortcuts and updated with the collected rewards. Thus, instead of storing the entire sequence of actions, the fly needs to compare only the values Q_1 and Q_2 for those shortcuts, thereby reducing the complexity of the representation of their habitat. We propose a tentative biological implementation of these two processes based on previous work. We speculate that dopamine signaling assigns values to spatial representations computed in central complex (idiothetic) or mushroom bodies (external cue-based navigation systems).

359 learning. In stable environments representations allow animals to take novel paths,
360 make short-cuts that save energy and minimize exposure to their predators. It is
361 worth noting that we did not manipulate external stimuli to disambiguate contribu-
362 tions of external or internal cues and therefore this remains an open question that
363 future studies can address.

364 However, in changing habitats animals need to learn new contingencies and,
365 therefore, foraging decisions need to incorporate learning processes. We show that a
366 simple Q-learning model [5] that uses both learning and forgetting rates for chosen
367 and unchosen options, respectively, can reproduce the return behavior of the flies.
368 Furthermore, we reveal the reinforcing effects of novelty and incorporate it into our
369 RL framework. The new finding [13] that dopamine neurons report novelty in flies
370 and the fact that at least some of these neurons mediate rewarding effect in flies [39]
371 is consistent with our findings that novelty itself is rewarding. Indeed reinforcing
372 effects of novelty might be a common driving force for exploration across species as
373 the same phenomenon was reported in rodents [40] and monkeys [41].

374 What do we gain by dissecting behaviors into multiple modules? First, we can see
375 if and how these modules interact at the level of behavior and reveal their hierarchical
376 structure. Second, it can inform us what type of connections exist at the neural level.
377 For example, if behavioral modules interact on the same level with antagonistic or
378 synergistic effects, this suggests mutual inhibitory or excitatory connections exists be-
379 tween brain areas that control behavioral expression of those modules. Alternatively,
380 if there are hierarchical dependencies this would suggest neuromodulatory influences.

381 According to our data, the RL system operates as a layer on top of the navigation-
382 based system and a neurobiological substrate in flies exists to suggest that the RL
383 system exerts neuromodulatory effects on the navigation-based system. The central
384 complex monitors angular orientation in fruit flies [42]. Both neural recordings [33,
385 43, 34] and behavioral manipulations [44] suggest that flies use a representation-
386 based navigation system. The neurons in the central complex (CX) express dopamine
387 receptors [45] and these neurons control angular motion in flies [46]. Therefore, the
388 navigation-based representations in CX can be updated (modulated) via a dopamine-
389 mediated reward prediction error that can implement model-based learning.

390 We note clear similarities of hierarchical and modular structure of behavioral
391 functions in flies and what has been first theorized and then experimentally tested in
392 humans. Some of the computational models in RL field explicitly distinguish model-
393 free and model-based learning systems [15]. The model-based RL framework [47]
394 suggests that the task structure and/or spatial representations are updated by reward

395 prediction error. This framework has been successfully used to explain hippocampus
396 dependent changes in choice strategy when human subjects were asked to make
397 decisions based on learned representations [48]. However, whether animals also rely
398 on model-based learning is an open question. Some of the studies in rodents are in
399 favor of such systems [49], yet extensive training protocols needed to achieve stable
400 performance in animals raises doubts whether model-based learning is replaced by
401 model-free learning system. Showing that navigation and learning systems cooperate
402 in fruit flies, our work is consistent with the idea these animals deploy model-based
403 learning to reduce the high dimensionality of the action space and achieve both
404 efficiency and adaptability.

405 Finally, we would like to caution against reductionism in behavioral neuroscience.
406 Recently it has been argued that neuroscience relies too much on a reductionist
407 bias [50] in understanding the link between the brain and behavior. Here we would
408 like to argue that behaviors themselves are subject to a reductionist bias by the desire
409 of the experimenter to place it within a single conceptual framework. Our approach
410 tried to break this trend and look at behaviors as composed of multiple modules,
411 be it reinforcement learning, cue-based navigation or innate and hard-wired foraging
412 strategies. We would like to argue that even in highly constrained environments set
413 to focus on a particular aspect of behavior, their inner multidimensional nature should
414 not be ignored but rather examined in detail [51]. Just to illustrate this point a recent
415 study by Stern et al [22] argued that a spatial task in flies is solved by trial-and-error
416 learning while Corfas et al [18] suggested that, in a very similar behavioral paradigm,
417 animals locate rewarding sites by using a path integration mechanism. We believe
418 that both strategies are indeed concurrently used in flies.

419 **Materials and Methods**

420 Single *Drosophila melanogaster* males were starved and placed in a linear track arena,
421 see Fig. 1A, which they were free to explore. The trehalose sugar-receptor neurons
422 *Gr5a* [23] were chosen to express the light-activated ion channel Channelrhodopsin
423 Chrimson [24], by means of the *LexA-LexAop* system. For details on fly strains and
424 rearing, see the supplementary methods section.

425 The optogenetic fly foraging setup consists of a 3d-printed platform with 12 linear
426 arenas of 5 by 50mm, each for a single fly, similar to Ref. [25]. The arenas are each
427 separated by black barriers to reduce visual contact to neighboring arenas. Red light
428 LEDs ($\lambda = 624(631)$ nm, Vishay VLCS5830) are mounted from below to illuminate

429 the respective region through a thin layer of plastic. The setup is surrounded sur-
430 rounded on three sides by acrylic panels (EndLighten, Acrylite), each lit by a strip of
431 white LEDs mounted along the end to provide white uniform background illumination
432 and a water reservoir for humidity. The setup is monitored from above with a webcam
433 (LifeCam Studio, Microsoft), fitted with a short-pass filter (FESH0600 Thorlabs) to
434 block red light from the stimulating LED. Centroid fly-tracking and stimulation are
435 controlled in an on-line fashion by custom written MATLAB (Mathworks) scripts. In
436 the camera view at the ends of each arena additional ROIs are defined to separate
437 'reward' and 'reset' zones. Using two zones allowed us to avoid self-stimulation when
438 the fly simply stayed in the rewarded location. The reward and reset zones extend
439 6 mm and 3 mm, respectively, and zones of the same type are of the same size.
440 Probabilistic rewards are triggered when the fly crosses the reset zone and enters the
441 reward zone, in that order. Refer to the inset of Fig. 1A for a depiction of the trigger
442 rule. The stimulation duration was 0.05 seconds.

443 **Fly Strains and Rearing** Flies were housed under a 12 h:12 h light:dark cycle at
444 25° C and 60–70% humidity on cornmeal, oatmeal, yeast and sucrose food. For all
445 experiments 3-6 day old males were used, which were starved for 10-12 h prior to
446 testing, while supplying water via a wet cloth. Flies were then transferred to the arena
447 using an aspirator and left in the arena for 2-10 hours. The following strains were
448 employed: *Gr5a-LexA* (gift from Kristin Scott [52]), *LexAop-Chrimson* ([24], w1118;
449 P{13XLexAop2-IVS-CsChrimson.mVenus} attP40, Bloomington 55138), *Canton S*
450 (from A.v.Philipsborn). The flies expressing *Chrimson* were fed all-trans retinal (ATR,
451 Sigma Aldrich, CAS Number: 116-31-4) for 2-3 days before the starvation period.
452 ATR food was prepared by mixing normal food with ATR to reach a 400 μ M solution
453 and then covered with aluminum foil to avoid degradation. Flies fed on ATR food
454 were kept in the dark under aluminum foil cover.

455 **Experimental Conditions** *Chrimson* > *Gr5a* flies were tested in eight different
456 single-sided stimulation conditions; with 0, 5, 15, 30, 45, 60, 75 and 100% stimulation
457 probability. In a second series of experiments, flies were tested under double-sided
458 stimulation conditions, with 5-5% and 15-15% stimulation probability.

459 **Post-processing of Walking Data** Walking traces were cleaned of missing data
460 points and jumps in the centroid contrast tracking and filtered with a butterworth
461 filter using a cutoff frequency determined from camera jitter. Next, a trial structure
462 was defined and data from flies with less than 50 trials was excluded from further
463 analysis.

464 **Definition of Observables** Stops were defined by speeds below a value of $|v| \leq$

465 0.01mm/s, which is governed by the resolution of our tracking system and corre-
466 sponds to a movement of less than one pixel between two timestamps. Turns were
467 defined by velocity sign changes since our setup is effectively one-dimensional.

468 **Logistic Regression** Regression analysis was performed on return choices against
469 their reward history for individual flies and fly populations by averaging over individu-
470 als from the same experimental condition. Due to the binary output variable we used
471 logistic regression. Here a weighted sum of the input variable $x_i, i \in \{1, \dots, M\}$
472 (reward history) is assumed to be a logit function of the dependent binary output
473 variable y (return choice). To estimate the weights β_i for each element of the reward
474 history, the weighted sum $h(x)$ is computed,

$$h(x) = \beta_0 + \sum_{i=1}^M \beta_i x_i \quad (2)$$

475 and used to define

$$y' = h(x) + \epsilon, \quad (3)$$

476 where ϵ is the remaining difference (error) between y' and the estimate of y', h . y' is
477 a continuous latent variable that needs to be mapped to the binary output variable
478 y . Thus, the probability of seeing $y = 1$ is a logistic function of h ,

$$P(y = 1) = \frac{1}{1 + e^{-h(x)}}. \quad (4)$$

479 Logistic regression yields estimates of the parameters β_i from the data which can be
480 used to make predictions.

481 To understand the values of the regression weights and what can be concluded about
482 the fly behavior from them, we generated 100000 element reward vectors with differ-
483 ent reward probabilities (5-30%). Under the assumption that the regression weights
484 are determined by how often the flies returned to a stimulation and neglecting any re-
485 ward correlations, we generated corresponding return choice vectors. The percentage
486 of return choices following a reward was set to approximate 'medium responsiveness',
487 with 50% correspondence. There were no choices on unrewarded trials. The regres-
488 sion weights can be seen in Fig. S3.

489

490 **Reinforcement Learning Models** The following reinforcement learning models [5]
491 were applied to the data to identify potential underlying algorithms: a Rescorla
492 Wagner (RW) model [6], a forgetting model where learning and forgetting rates
493 are equal (termed FQ model) and a forgetting model where learning and forgetting

494 happen at different rates (termed FQ^{α_F}).

495 The RL models were fit to each individual fly using maximum likelihood estimation
496 with the following log likelihood function

$$L = \frac{1}{N} \sum_{t=1}^N \left((1 - c(t)) \cdot \log(1 - P(c(t) = 1)) + c(t) \cdot \log P(c(t) = 1) \right). \quad (5)$$

497 $c(t) = 1$ corresponds to a return choice and $c(t) = 0$ corresponds to no choice on trial
498 t . The simple RW model has three parameters, α , β and *bias*, where α is the learning
499 rate, determining the impact of the reward-prediction error, $R(t) - Q(t - 1)$, on the
500 value update, where $R(t)$ is the reward at trial t and $Q(t)$ is the value corresponding
501 to a choice. β is the weighting factor of the value in the choice probability,

$$P(c(t) = 1) = \frac{1}{1 + e^{\beta(\textit{bias} - Q(t))}}. \quad (6)$$

502 A *bias* parameter was included, to account for the fact that the baseline return
503 probability for a fly is below 50%. In this simple model, the value of a choice $c = 1$ is
504 only updated, when the fly made a choice, and remains constant otherwise ($\phi = 0$ in
505 Eq.). To make the model slightly more realistic, a second RL model, the FQ model,
506 was implemented, where the value of a choice was forgotten, if the fly didn't make
507 a choice, with the same learning parameter $\phi = \alpha$ as in the value update equation.
508 The third model had one additional parameter, a forgetting parameter $\phi = \alpha_F$, to
509 allow for the more general case of different strengths of the learning and forgetting
510 processes.

$$Q^{\text{FQ}}(t) = \begin{cases} Q^{\text{FQ}}(t - 1) + \alpha(R(t) - Q^{\text{FQ}}(t - 1)), & \text{if } c(t) = 1 \\ Q^{\text{FQ}}(t - 1) - \phi Q^{\text{FQ}}(t - 1), & \text{else.} \end{cases} \quad (7)$$

511 Every fly was fit with 100 random initializations of these parameter sets for each
512 model and the best parameters were selected by the corresponding highest log likeli-
513 hood values, $\ln(L)$. Subsequently, the Akaike Information Criterion [53] (AIC) score
514 was computed, to select the one that best fits the data, while taking the number of
515 parameters into account.

516 To allow for predictive testing of the models, only half of every fly data was used
517 to fit the parameter values and the other half was used to predict the flies' choices.

518 The F_1 score was used as accuracy measure for every fly,

$$\text{precision} = \text{TP}/(\text{TP} + \text{FP}) \quad (8)$$

$$\text{recall} = \text{TP}/(\text{TP} + \text{FN}) \quad (9)$$

$$F_1 = 2 \frac{\text{precision} \cdot \text{recall}}{\text{precision} + \text{recall}}, \quad (10)$$

519 with TP the rate of true positives, FP the rate of false positives and FN the rate of
520 false negatives.

521 To test the models' generative power, 1000 sequences of 1000 trials each for the
522 different experimental probability conditions were simulated.

523 Acknowledgement

524 This study was supported by Lundbeckfonden grant no. DANDRITE-R248-2016-
525 2518. We gratefully acknowledge helpful comments from Dennis Eckmeier, Alex
526 Gomez-Marin, Daisuke Hattori and Ollie Hulme.

527 Author Contributions

528 JIS and DK designed the experiment. SES performed all experiments and analyses.
529 SES and DK wrote the manuscript. ACvP provided expertise and feedback.

530 References

531

532 [1] Ploeger A, Galis F. Evo devo and cognitive science. Wiley Interdisciplinary Re-
533 views: Cognitive Science. 2011 Jul;2(4):429-40.

534 [2] Tinbergen N. The hierarchical organization of nervous mechanisms underlying
535 instinctive behavior. Foundations of animal behavior: Classic papers with com-
536 mentaries. 1996;406:413.

537 [3] Behrens TE, Woolrich MW, Walton ME, Rushworth MF. Learning the value of
538 information in an uncertain world. Nat Neurosci. 2007 Sep;10(9):1214-21

- 539 [4] Schultz W, Preuschoff K, Camerer C, Hsu M, Fiorillo CD, Tobler PN, Bossaerts
540 P. Explicit neural signals reflecting reward uncertainty. *Philos Trans R Soc Lond B*
541 *Biol Sci*. 2008 Dec 12;363(1511):3801-11.
- 542 [5] R. S. Sutton, and A. G. Barto, *Reinforcement learning: an introduction*, MIT
543 Press, 1998.
- 544 [6] R. A. Rescorla, A. R. Wagner, *A theory of Pavlovian conditioning: Variations in*
545 *the effectiveness of reinforcement and nonreinforcement* in *Classical Conditioning*
546 *II: Current Research and Theory* (Eds. A. H. Black, W. F. Prokasy), Appleton
547 Century Crofts, 1972.
- 548 [7] Brea J, Urbanczik R, Senn W. A normative theory of forgetting: lessons from
549 the fruit fly. *PLoS Comput Biol*. 2014 Jun 5;10(6)
- 550 [8] Berry JA, Cervantes-Sandoval I, Nicholas EP, Davis RL. Dopamine is required for
551 learning and forgetting in *Drosophila*. *Neuron*. 2012 May 10;74(3):530-42
- 552 [9] Friston KJ, Daunizeau J, Kiebel SJ. Reinforcement learning or active inference?
553 *PLoS One*. 2009 Jul 29;4(7):
- 554 [10] Schultz W. Dopamine reward prediction-error signalling: a two-component re-
555 sponse. *Nat Rev Neurosci*. 2016 Mar;17(3):183-95
- 556 [11] Cavigelli SA, Michael KC, West SG, Klein LC. Behavioral responses to physical
557 vs. social novelty in male and female laboratory rats. *Behav Processes*. 2011
558 Sep;88(1):56-9.
- 559 [12] Kakade S, Dayan P. Dopamine: generalization and bonuses. *Neural Netw*. 2002
560 Jun-Jul;15(4-6):549-59
- 561 [13] Hattori D, Aso Y, Swartz KJ, Rubin GM, Abbott LF, Axel R. Representations
562 of Novelty and Familiarity in a Mushroom Body Compartment. *Cell*. 2017 May
563 18;169(5):956-969
- 564 [14] Tse, Dorothy, et al. "Schema-dependent gene activation and memory encoding
565 in neocortex." *Science* 333.6044 (2011): 891-895.
- 566 [15] Daw, Nathaniel D and Dayan, Peter, The algorithmic anatomy of model-based
567 evaluation, *Philosophical Transactions of the Royal Society B: Biological Sci-*
568 *ences*,369,1655,20130478,(2014)

- 569 [16] I. Kim, M. Dickinson, Idiothetic path integration in the fruit fly *Drosophila*
570 *melanogaster*, *Current Biology*, 2017.
- 571 [17] Ofstad TA, Zuker CS, Reiser MB. Visual place learning in *Drosophila*
572 *melanogaster*. *Nature*. 2011 Jun 8;474(7350):204-7.
- 573 [18] Corfas RA, Sharma T, Dickinson MH. Diverse food-sensing neurons trigger
574 idiothetic local search in *Drosophila*. *Current Biology*. 2019 May 20;29(10):1660-
575 8.
- 576 [19] R. Wehner, B. Michel, and P. Antonsen, *navigation in insects: coupling of*
577 *egocentric and geocentric information*, *Journal of Experimental Biology* **199**, 1
578 (1996)
- 579 [20] Bell, William J. "Searching behavior patterns in insects." *Annual review of en-*
580 *tomology* 35.1 (1990): 447-467
- 581 [21] Haberkern H, Basnak MA, Ahanonu B, Schauder D, Cohen JD, Bolstad M,
582 Bruns C, Jayaraman V. Visually guided behavior and optogenetically induced
583 learning in head-fixed flies exploring a virtual landscape. *Current Biology*. 2019
584 May 20;29(10):1647-59.
- 585 [22] Stern U, Srivastava H, Chen HL, Mohammad F, Claridge-Chang A, Yang CH.
586 Learning a Spatial Task by Trial and Error in *Drosophila*. *Curr Biol*. 2019 Aug
587 5;29(15):2517-2525
- 588 [23] S. Chyb, A. Dahanukar, A. Wickens, and J. R. Carlson, *Drosophila Gr5a encodes*
589 *a taste receptor tuned to trehalose*, *Proc. Natl. Acad. Sci. USA*. **100**, 14526
590 (2003).
- 591 [24] N. C. Klapoetke, Y. Murata, S. S. Kim, S. R. Pulver, A. Birdsey-Benson,
592 Y. K. Cho, T. K. Morimoto, A. S. Chuong, E. J. Carpenter, Z. Tian, J. Wang,
593 Y. Xie, Z. Yan, Y. Zhang, B. Y. Chow, B. Surek, M. Melkonian, V. Jayaraman,
594 M. Constantine-Paton, G. Ka-Shu Wong, and E. S. Boyden, *Independent optical*
595 *excitation of distinct neural populations*, *Nat. Methods*. **11**, 338 (2014).
- 596 [25] K. Steck, D. Veit, R. Grandy, S. Bermudez i Badia, Z. Mathews, P. Verschure,
597 B. S. Hansson, and M. Knaden, *A high-throughput behavioral paradigm for*
598 *Drosophila olfaction - the flywalk*, *Sci. Rep.* **2**, 361 (2012).

- 599 [26] Claridge-Chang A, Roorda RD, Vrontou E, Sjulson L, Li H, Hirsh J, Miesenböck
600 G. Writing memories with light-addressable reinforcement circuitry. *Cell*. 2009 Oct
601 16;139(2):405-15
- 602 [27] A. Brockmann, P. Basu, M. Shakeel, S. Murata, N. Murashima, R. K. Boyapati,
603 N. G. Prabhu, J. J. Herman, and T. Tanimura, *Sugar intake elicits intelligent*
604 *searching behavior in flies and honey bees*, *Front. Behav. Neurosci.* **12**, 280
605 (2018).
- 606 [28] Lau, Brian, and Paul W. Glimcher. "Dynamic response-by-response models of
607 matching behavior in rhesus monkeys." *Journal of the experimental analysis of*
608 *behavior* 84.3 (2005): 555-579.
- 609 [29] Hwang, Eun Jung, et al. "History-based action selection bias in posterior parietal
610 cortex." *Nature communications* 8.1 (2017): 1242.
- 611 [30] Akaishi, Rei, et al. "Autonomous mechanism of internal choice estimate under-
612 lies decision inertia." *Neuron* 81.1 (2014): 195-206.
- 613 [31] Brembs B, Heisenberg M. The operant and the classical in conditioned ori-
614 entation of *Drosophila melanogaster* at the flight simulator. *Learn Mem.* 2000
615 Mar-Apr;7(2):104-15.
- 616 [32] Pernet, C.R., Wilcox, R. & Rousselet, G.A. (2013). Robust correlation analyses:
617 false positive and power validation using a new open source Matlab toolbox.
618 *Front. in Psychology*, 3, 606.
- 619 [33] Green J, Adachi A, Shah KK, Hirokawa JD, Magani PS, Maimon G. A
620 neural circuit architecture for angular integration in *Drosophila*. *Nature*. 2017
621 Jun;546(7656):101.
- 622 [34] Turner-Evans D, Wegener S, Rouault H, Franconville R, Wolff T, Seelig JD,
623 Druckmann S, Jayaraman V. Angular velocity integration in a fly heading circuit.
624 *Elife*. 2017 May 22;6:e23496.
- 625 [35] Mizunami M, Weibrecht JM, Strausfeld NJ. Mushroom bodies of the cockroach:
626 their participation in place memory. *Journal of Comparative Neurology*. 1998 Dec
627 28;402(4):520-37.

- 628 [36] Brockmann A, Basu P, Shakeel M, Murata S, Murashima N, Boyapati RK,
629 Prabhu NG, Herman JJ, Tanimura T. Sugar intake elicits intelligent searching
630 behavior in flies and honey bees. *Frontiers in behavioral neuroscience*. 2018;12.
- 631 [37] Tortorici C, Brody A, Bell WJ. Influence of spatial patterning of resources on
632 search orientation of adult *Drosophila melanogaster*. *Anim Behav* 1986; 34:1568-
633 70.
- 634 [38] Nuwal N, Stock P, Hiemeyer J, Schmid B, Fiala A, Buchner E. Avoidance of heat
635 and attraction to optogenetically induced sugar sensation as operant behavior in
636 adult *Drosophila*. *J Neurogenet*. 2012 Sep;26(3-4):298-305.
- 637 [39] Lin S, Oswald D, Chandra V, Talbot C, Huetteroth W, Waddell S. Neural
638 correlates of water reward in thirsty *Drosophila*. *Nature neuroscience*. 2014
639 Nov;17(11):1536.
- 640 [40] Menegas W, Babayan BM, Uchida N, Watabe-Uchida M. Opposite initialization
641 to novel cues in dopamine signaling in ventral and posterior striatum in mice. *Elife*.
642 2017 Jan 5;6:e21886.
- 643 [41] Bromberg-Martin ES, Matsumoto M, Hikosaka O. Dopamine in motivational
644 control: rewarding, aversive, and alerting. *Neuron*. 2010 Dec 9;68(5):815-34.
- 645 [42] Turner-Evans DB, Jayaraman V. The insect central complex. *Current Biology*.
646 2016 Jun 6;26(11):R453-7.
- 647 [43] Kim SS, Rouault H, Druckmann S, Jayaraman V. Ring attractor dynamics in
648 the *Drosophila* central brain. *Science*. 2017 May 26;356(6340):849-53.
- 649 [44] Green J, Vijayan V, Pires PM, Adachi A, Maimon G. A neural heading estimate is
650 compared with an internal goal to guide oriented navigation. *Nature neuroscience*.
651 2019 Jul 22:1-9.
- 652 [45] Kong EC, Woo K, Li H, Lebestky T, Mayer N, Sniffen MR, Heberlein U, Bainton
653 RJ, Hirsh J, Wolf FW. A pair of dopamine neurons target the D1-like dopamine
654 receptor DopR in the central complex to promote ethanol-stimulated locomotion
655 in *Drosophila*. *PLoS one*. 2010 Apr 1;5(4):e9954.
- 656 [46] Kottler B, Faville R, Bridi JC, Hirth F. Inverse Control of Turning Behavior by
657 Dopamine D1 Receptor Signaling in Columnar and Ring Neurons of the Central
658 Complex in *Drosophila*. *Current Biology*. 2019 Feb 18;29(4):567-77.

- 659 [47] Daw ND, Niv Y, Dayan P. Uncertainty-based competition between prefrontal
660 and dorsolateral striatal systems for behavioral control. *Nature neuroscience*. 2005
661 Dec;8(12):1704.
- 662 [48] Vikbladh OM, Meager MR, King J, Blackmon K, Devinsky O, Shohamy D,
663 Burgess N, Daw ND. Hippocampal contributions to model-based planning and
664 spatial memory. *Neuron*. 2019 May 8;102(3):683-93.
- 665 [49] Miller KJ, Botvinick MM, Brody CD. Dorsal hippocampus contributes to model-
666 based planning. *Nature neuroscience*. 2017 Sep;20(9):1269.
- 667 [50] Krakauer, John W., et al. "Neuroscience needs behavior: correcting a reduc-
668 tionist bias." *Neuron* 93.3 (2017): 480-490.
- 669 [51] Alex Gomez-Marin, Asif A. Ghazanfar. The Life of Behavior. *Neuron*. Volume
670 104, Issue 1,2019,Pages 25-36,
- 671 [52] M. D. Gordon and K. Scott, *Motor control in a Drosophila taste circuit*, *Neuron*
672 **61**, 373 (2009).
- 673 [53] H. Akaike, *Information theory and an extension of the maximum likelihood*
674 *principle*, Proceedings of the 2nd International Symposium on Information Theory
675 (Eds. B. N. Petrov and F. Csaki), 1973.

676 **Supplementary Information**

677 **Supplementary Figure 1**

678 The optogenetic stimulation changes the walking patterns of the flies, from a more
679 uniform positional coverage of the arena, to a stimulation zone localized occupancy
680 (Fig. S1A,B). The speed distribution of genetic and unstimulated control flies is
681 bimodal, with a slow peak from wall approach and a fast peak from walking in
682 the inner part of the arena, which is also (but to a lesser degree) preserved on the
683 unrewarded trials of the stimulated populations (Fig. S1A left). Upon stimulation,
684 the fast peak is decreased and the slow peak slightly increased (Fig. S1A. right). The
685 average walking speed is similar across conditions and strongly reduced in contrast to
686 freely walking flies [1], due to the confinement (Fig. S1D). To characterize the trials
687 we imposed on the data, we looked at the trial length distributions of stimulated and
688 unstimulated trials. Fig. S1C shows 4 example conditions and their population trial
689 length distributions. Stimulated or rewarded trials were longer due to the lingering
690 time from experiencing the reward and the subsequent local search like behavior.
691 The distributions are similar across probability conditions, indicating that the arena
692 geometry and thereby the walking speed are imposing boundaries on the typical
693 duration of a trial. Since the population speed distributions in Fig. S1A didn't show
694 a very clear effect of the stimulation on the walking speed, we looked at the local
695 walking speed distribution of the flies after they received a reward. When walking out
696 of the stimulation zone, the flies showed a fast peak, while when they then returned
697 to the stimulation zone, the speed was reduced (Fig. S1D). This effect was averaged
698 out in the population speed distribution.

699 **Supplementary Figure 2**

700 In addition to the single sided experiments, we also collected double-sided stimulation
701 data in two conditions, 5:5% and 15:15%. We performed the same analysis on this
702 data as on the single-sided data. The occupancy distribution showed peaks in both
703 stimulated zones (Fig. S2A) and the zone preference indices were close to zero in
704 both cases, indicating no preference for one zone over the other (Fig. S2B). The
705 returns to both zones were not significantly different and similar to those of the
706 single-sided conditions of the same probability (Fig. S2C). Since the first reward
707 could happen in either zone, we compared first reward return probabilities to both
708 zones for the two double-sided conditions (Fig. S2D left) and the corresponding first

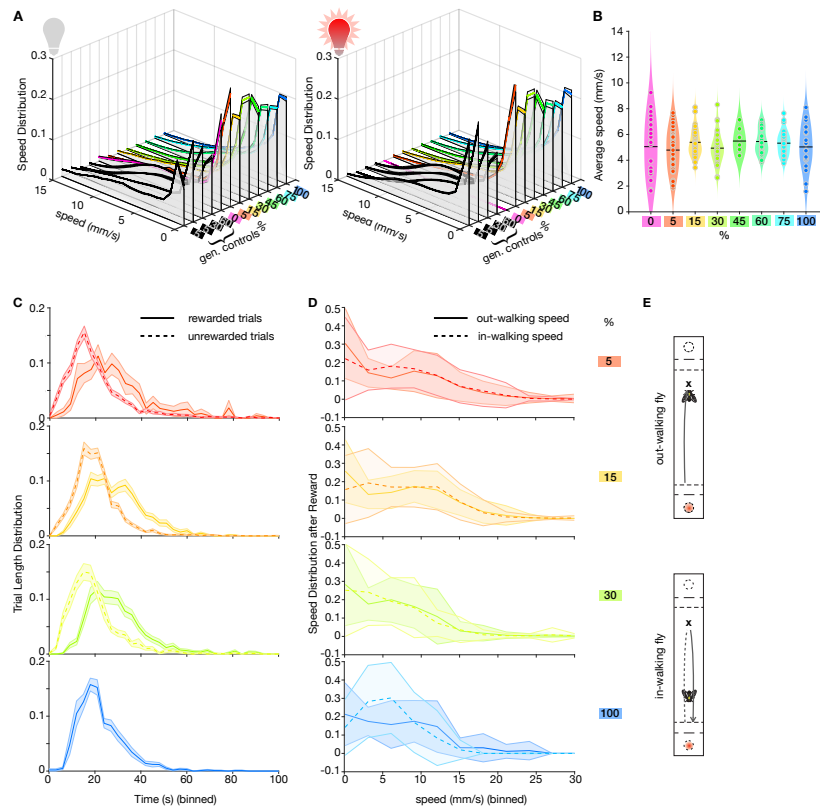


Figure S1: Population speed and Characterization of Trials. **A** Speed distribution of fly populations. Left: unstimulated trials (grey light bulb). Right: stimulated trials (red light bulb). Stimulation affects the higher speeds but not the low speeds. **B** Average walking speed per condition. **C** Trial length distribution of 5,15,30 and 100% condition populations. Solid lines show rewarded trials (longer) and dashed lines show unrewarded trials (shorter). **D** Speed distribution after a reward. Solid lines: out of the reward zone walking speed. Dashed lines: in-walking speed when returning from walking out (same trial as out-walking speed). In-walking is on average slower than out-walking. **E** Pictogram of out-walking and in-walking traces.

709 rewarded trial numbers (Fig. S2D right). Both were consistent with the results from
 710 the single-sided cases. Logistic regression analysis (Fig. S2E) revealed again that the
 711 current reward was most predictive of a return and that there was no influence of the
 712 return history. To test whether the animals also followed a reinforcement learning
 713 algorithm to allocate their choices to two options, we used the same three types
 714 of models, extended by a second option. Model comparison (Fig. S2H) yielded the
 715 lowest AIC score for the FQ model, which captured return probabilities to both zones,
 716 as well as return run lengths in both probability conditions in a generative test, well
 (Fig. S2J,K).

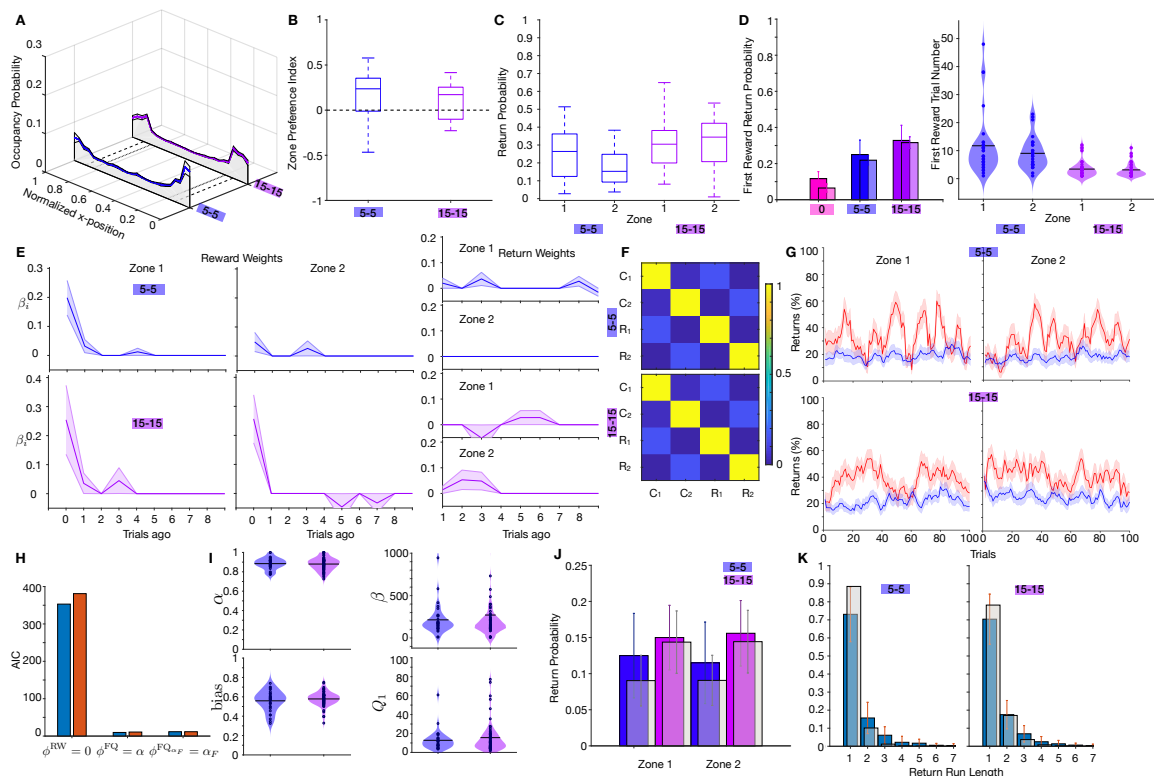


Figure S2: Experiments with double-sided stimulation. **A** Occupancy distribution for 5% and 15% double-sided stimulation data. **B** Preference index. **C** Return probability to zones 1 and 2 for both conditions. **D** Left: Return behavior on the first reward (to either zone) compared to the first trial return for unstimulated controls. Right: First rewarded trial number. **E** Left and center: Logistic regression weights of returns against the reward history for both population data to each zone independently. Right: Logistic regression weights for returns against return choice history. **F** Pearson correlation for rewards (R) and returns (C). **G** Return behavior as 5-trial moving average. Red curves: rewarded trials, blue curves: unrewarded trials to the same zone. **H** AIC score for the three RL models. **I** Best-fit parameter values of the FQ model. **J** Generative testing of the FQ model: comparison of the return probability (exp. data: colored, model: grey). **K** Generative testing of the FQ model: Return run lengths (exp. data: blue, model: grey).

717

718 **Supplementary Figure 3**

719 We concluded that the flies perform local searches after receiving a reward since their
720 turns increase around the reward location. How do those distributions look in time
721 after a reward? Fig. S3A shows population averaged turns for individual rewarded
722 (upper row) and unrewarded (bottom row) trials in time since a trial start at $t = 0$.
723 Each local search time was cutoff at the time of the return to the reward zone. To
724 capture the general time course, both scatter plots are summarized as histograms
725 in the middle row. Comparing those distributions shows that rewarded flies perform
726 more temporally extended curved trajectories than unstimulated flies. We performed
727 the same analysis on the time points of returns, Fig. S3B and revealed that, if they
728 return, unstimulated trials are returned faster than rewarded trials, consistent with
729 a more extended local search behavior after a reward. Are those local searches
730 a hard-wired behavior that is always elicited upon reward encounter (specifically
731 sweet taste rewards) or do they undergo adaptation to the reward probability? To
732 test this, we show polar plots of the angular distribution of the walking paths in
733 the reset zone in Fig. S3C. Rewarded (solid lines) and unrewarded (dashed lines)
734 trials separate in this visualization, since the search path has a larger variability
735 in turn angles than an unrewarded fly's path, that only turns at the arena wall.
736 While they are significantly different within the probability condition, the angular
737 distributions on rewarded trials across probability conditions are not. Furthermore,
738 the unrewarded angular distributions across conditions are significantly different from
739 the unstimulated control flies (0%). Together, this suggests that local searches
740 emerge upon reward encounter, they are hard-wired in the sense that they are not
741 different across probability conditions and unrewarded trials actually have less 'curvy'
742 paths than those of always unstimulated flies. Providing a second reward location,
743 as in the double-sided conditions, can help elucidate whether the flies localize their
744 returns in space to the availability of rewards in zone 2 of the arena. We compared
745 the distribution of returns in space from the reward zone for the 5 and 15% single
746 and double-sided data, Fig. S3D. In all conditions, the flies are more likely to return
747 spatially close to the previously visited reward zone and the probability decreases
748 the further away the fly walks. There was no difference between the single- and
749 double-sided conditions, rejecting our hypothesis of return localization.

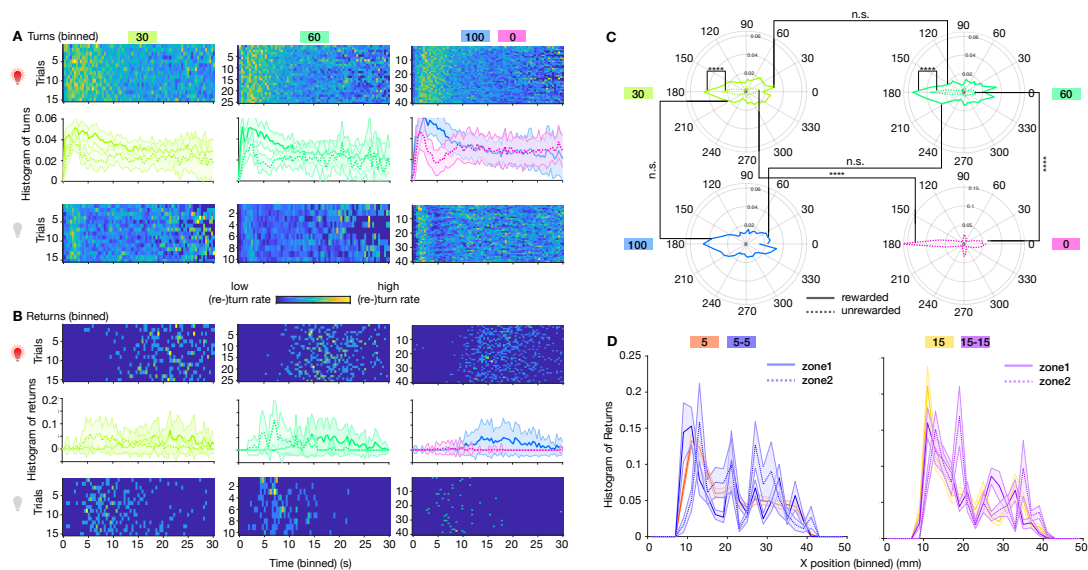


Figure S3: Local search analysis **A** Top row: Turns, as a proxy for local search, (binned) in time since trial start for 30, 60 and 100/0% conditions. Middle row: histogram of temporal turn distribution. Solid drawn curve corresponds to rewarded trials (top row) and dashed curve corresponds to unstimulated trials (bottom row). Bottom row: turns in time since trial start for unstimulated trials. **B** Top row: returns on rewarded trials in time since trial start for the same fly populations. Middle row: histogram of returns. Solid curve: stimulated returns, dashed curve: unstimulated returns. Bottom row: Unstimulated returns. **C** Polar plots of angular distributions of walking traces in the reset zone, for 30%, 60%, 100% populations and unstimulated controls (clockwise). Solid lines: rewarded trials, dashed lines: unrewarded trials. (***) : $p < 0.0001$, two-way Kolmogorov-Smirnoff test.) **D** Comparison of return location (maximum position of a trial) for 5 and 15% single and double sided condition fly populations. Double sided cases have rewards in both zones and thus returns to both zones are separated.

750 Supplementary Figure 4

751 To determine how stable the return behavior was over the time of the session, we
 752 looked at 5-trial moving averages of the returns for the fly populations in each
 753 probability condition (Fig. S4A). With increasing stimulation probability, the returns
 754 upon rewards (red curves in Fig. S4A) decreased over time (trials). The data shown
 755 corresponds to 2 hours of experiment. We therefore reduced the data to 30 minutes
 756 where the return behavior was approximately stable for all conditions. To justify
 757 the regression analysis we looked at the pearson correlation of the rewards and the
 758 animals' returns (Fig. S4B). To help interpret the logistic regression weights, we
 759 simulated rewards with 5 different reward probabilities (5-30%) and return vectors,
 760 where the return probability upon a reward was set to 50% (Fig. S4C). The size of
 761 the first coefficient was thus determined by the stimulation probability and explains
 762 the effect we see in Fig. 2D.

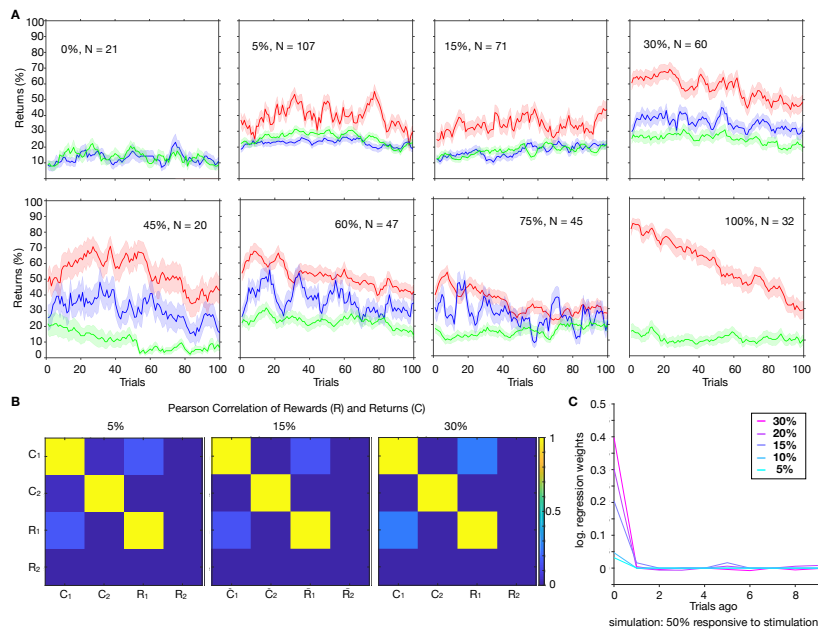


Figure S4: Stability of return behavior over trials and reward-choice correlations. **A** 5-trial moving averages of the returns over trials for 0-100% stimulation probability conditions. Red curves show returns upon rewards, blue curves show returns to the rewarded zone without rewards and green curves show returns to the unstimulated zone. **B** Pearson correlation of rewards and returns (choices) for 5,15 and 30% conditions. **C** Logistic regression of simulated data to rewards. Simulated data was generated with 50% return probability upon a reward. Curves show regression weights for different stimulation probabilities (5-30%).

763 Supplementary Figure 5

764 We tested three reinforcement learning models (see also Sec.) and compared their
 765 AIC scores as a measure of how well they captured the data (Fig. S5A). The models
 766 were fit on half of the data (of each fly) and the other half was used to perform
 767 a predictive test (Fig. S5C). Especially the low probability data could not be very
 768 well predicted, which is due to the limited number of reward and return events in the
 769 data. This is visualized in Fig. S5D by means of the F_1 score, a measure of predictive
 770 accuracy against the probability of returned trials. Data with more returns could be
 771 fit more reliably and yielded a higher F_1 accuracy. The slightly better predictive
 772 performance of the FQ model than the RL model made us choose this model to
 773 explain the return behavior. The corresponding best-fit parameters of the flies whose
 774 behavior could be predicted by the FQ model, are shown in Fig. S5B. We furthermore
 775 used the models for generative testing, where we used the return probability and the
 776 return run length distributions as measures for comparison with the experimental
 777 data. All models perform well and generate distributions quite close to that of the
 778 exp. data.

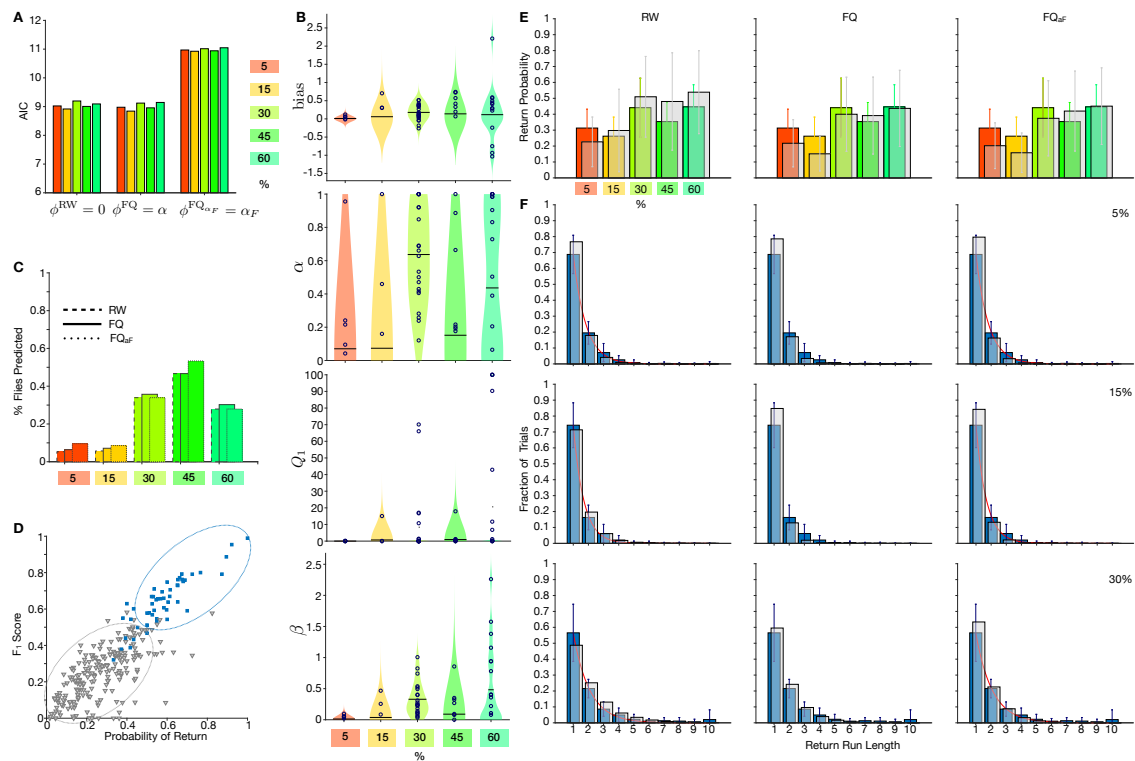


Figure S5: Reinforcement learning model selection, predictive test and generative test. **A** AIC scores for the three RL models on 5-60% data. The lower the AIC score, the better the model captures the data while excessive parameters are punished. **B** Best-fit parameter values of the FQ model for each fly (circles) and population averages (solid lines in the violins). **C** Predictive test of the FQ model. Number of flies that could be predicted with more than 50% accuracy (F_1 score) for each model. Total number of flies per condition: $N^{5\%} = 94$, $N^{15\%} = 70$, $N^{30\%} = 56$, $N^{45\%} = 15$, $N^{60\%} = 45$. **D** F_1 score against data choice probability. If choices made up less than 50% of the data, the model had a poor predictive power. Dashed ellipses visualize clustering of the data with high and low F_1 score. **E** Comparison of generative properties of the three RL models: Return probability. **F** Comparison of generative properties of the three RL models: Return run lengths. Red curves: exponential fits.

779 References

780

- 781 [1] C. S. Mendes, I. Bartos, T. Akay, S. Márka, and R. S. Mann, *Quantification*
 782 *of gait parameters in freely walking wild type and sensory deprived Drosophila*
 783 *melanogaster*, eLife 2, e00231 (2013).